

iScience, Volume 23

Supplemental Information

Tumor Microenvironment-Activated Degradable Multifunctional Nanoreactor for Synergistic Cancer Therapy and Glucose SERS Feedback

Dan Sun, Guohua Qi, Kongshuo Ma, Xiaozhang Qu, Weiqing Xu, Shuping Xu, and Yongdong Jin

Supporting information

Tumor Microenvironment Activated Degradable Multifunctional Nanoreactor for Synergistic Cancer Therapy and Glucose SERS

Feedback

Dan Sun,^{1,#} Guohua Qi,^{2,#} Kongshuo Ma,^{2,3} Xiaozhang Qu,¹ Weiqing Xu,¹ Shuping Xu,^{1,*} Yongdong Jin^{2,3,*}

¹ State Key Laboratory of Supramolecular Structure and Materials, Institute of Theoretical Chemistry, College of Chemistry, Jilin University, Changchun 130012, P. R. China.

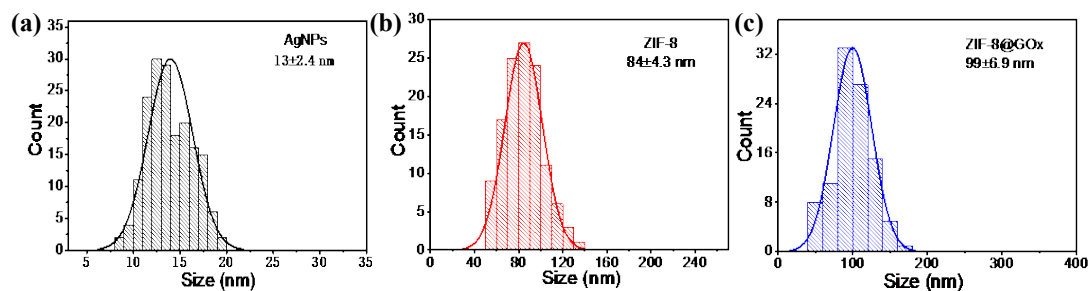
² State Key Laboratory of Electroanalytical Chemistry, Changchun Institute of Applied Chemistry, Chinese Academy of Sciences, Changchun 130022, Jilin, P. R. China.

³ University of Science and Technology of China, Hefei 230026, P. R. China.

[#] Dan Sun and Guohua Qi contributed equally to this article.

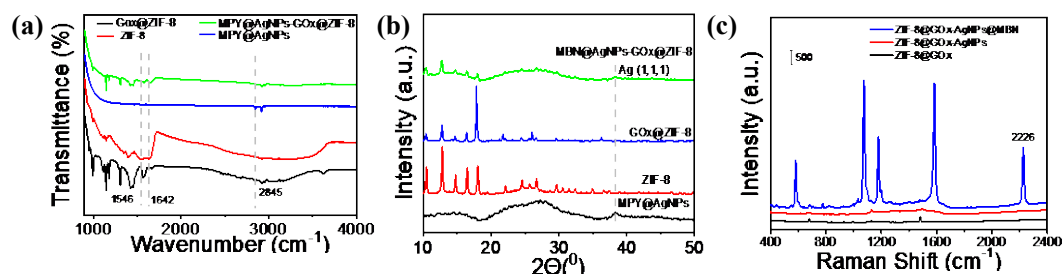
^{*} Correspondence: xusp@jlu.edu.cn (X. S.), ydjn@ciac.ac.cn (J. Y.)

1. Characterizations of the ZIF-8@GOx-AgNPs@MBN



Supplemental Figure 1: Related to Figure 1

Figure S1. The statistic particle sizes of (a) AgNPs, (b) ZIF-8 and (c) ZIF-8@GOx, respectively, used in this study.



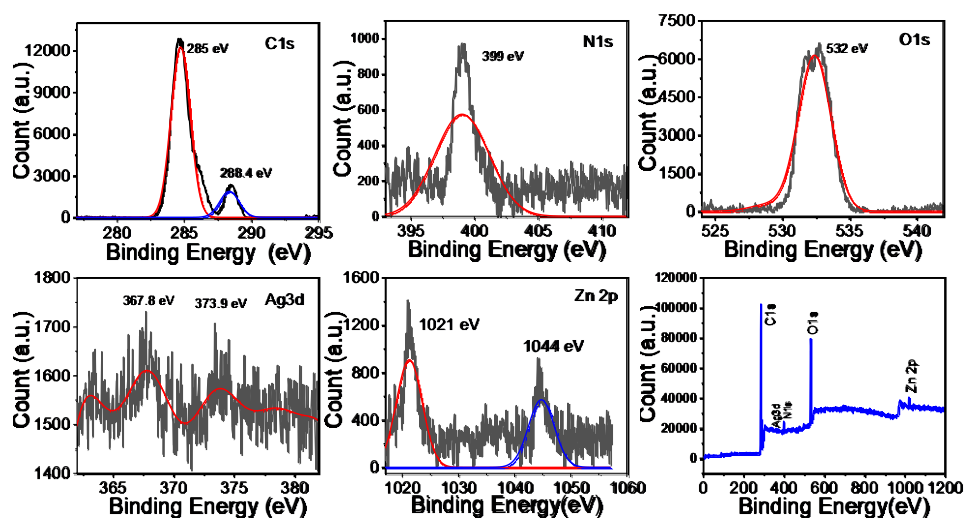
Supplemental Figure 2: Related to Figure 1

Figure S2. (a) FT-IR spectra and (b) XRD patterns of the AgNPs@MBN, ZIF-8, ZIF-8@GOx, and the ZIF-8@GOx-AgNPs@MBN nanoreactors, respectively. (c) SERS spectra of ZIF-8@GOx, ZIF-8@GOx-AgNPs, and the nanoreactors, respectively. A laser wavelength of 632.8 nm and an acquisition time of 5 s were used for the SERS measurements.

Figure S2 shows the FTIR analysis of the AgNPs@MBN, ZIF-8, ZIF-8@GOx, and the ZIF-8@GOx-AgNPs@MBN. By comparison FT-IR spectrum of the nanoreactors with others (Figure S2), we can find that the bands from ~2840 to 2850 cm⁻¹ and from ~1630 to 1650 cm⁻¹, ascribed to the amide I and II bands respectively, are identified, indicating the successful fixing of the AgNPs@MBN on the surface of ZIF-8@GOx.

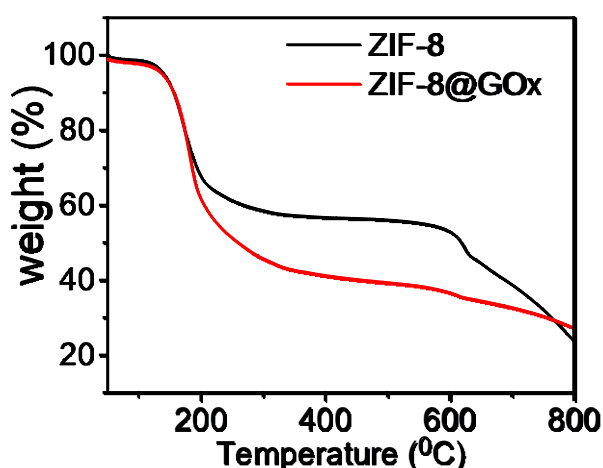
Moreover, the XRD data confirm that the ZIF-8@GOx maintained the same crystalline form as the pure ZIF-8 NPs (Figure S2b), suggesting that the hybridization preparation did not alter the crystalline structure of ZIF-8. Moreover, the peaks of ZIF-8@GOx-AgNPs@MBN centered at 8.3°, 18.4° and 28.3°, 30.4° indicate the

co-existence of the standard Bragg reflections of ZIF-8 and metallic AgNPs (e.g., 111, 200), testifying again the complex structure of the ZIF-8@GOx-AgNPs@MBN.



Supplemental Figure 3: Related to Figure 1

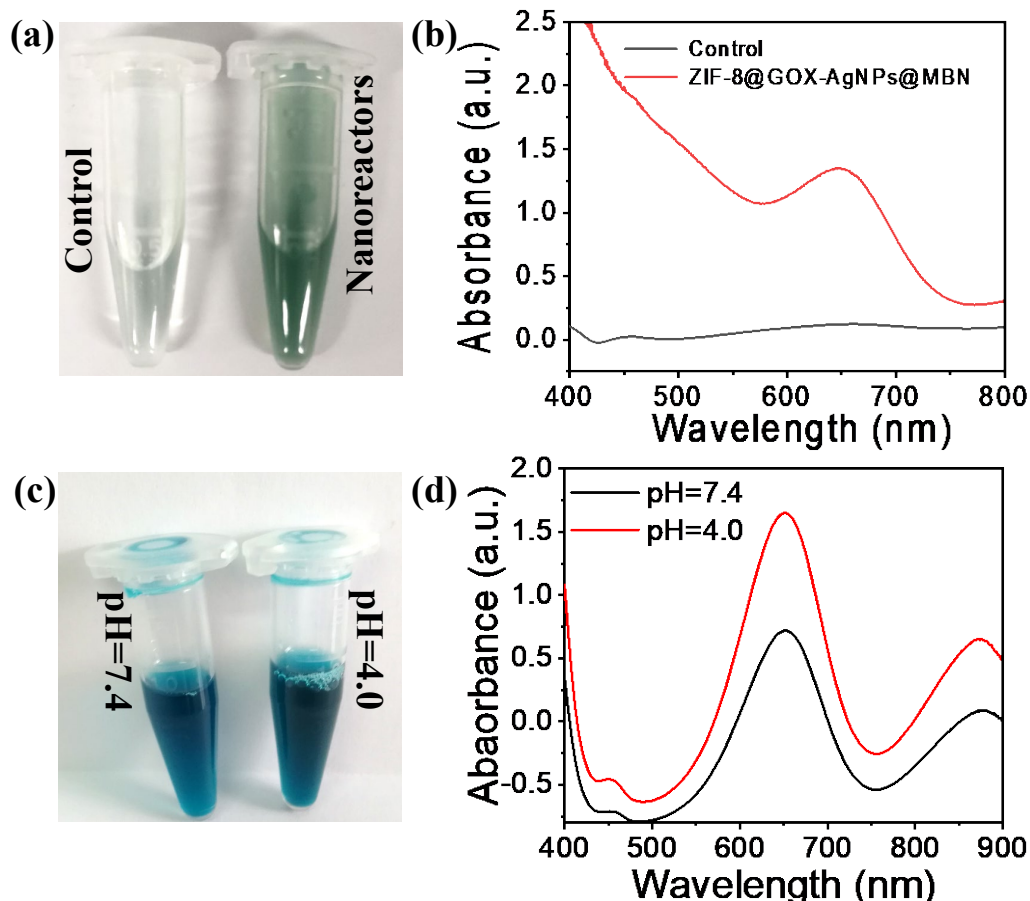
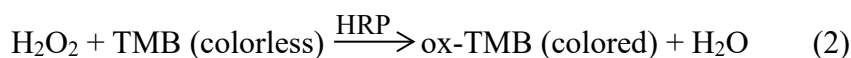
Figure S3. The XPS spectra of C 1s, N 1s, O 1s, Ag 3d, and Zn 2p of the nanoreactor, respectively. The XPS spectra were carried out to analyze the valence state of the elements of the ZIF-8@GOx-AgNPs@MBN nanoreactor. The peaks located at 285 eV and 288.4 eV are attributed to C 1s and the peaks at 399 and 532 eV belong to N 1s and O 1s, respectively. The peak located at 1044 eV is Zn 2p of the ZIF-8 (Figure S3).



Supplemental Figure 4: Related to Figure 1

Figure S4. Thermogravimetric analysis (TGA) of ZIF-8 and ZIF-8@GOx.

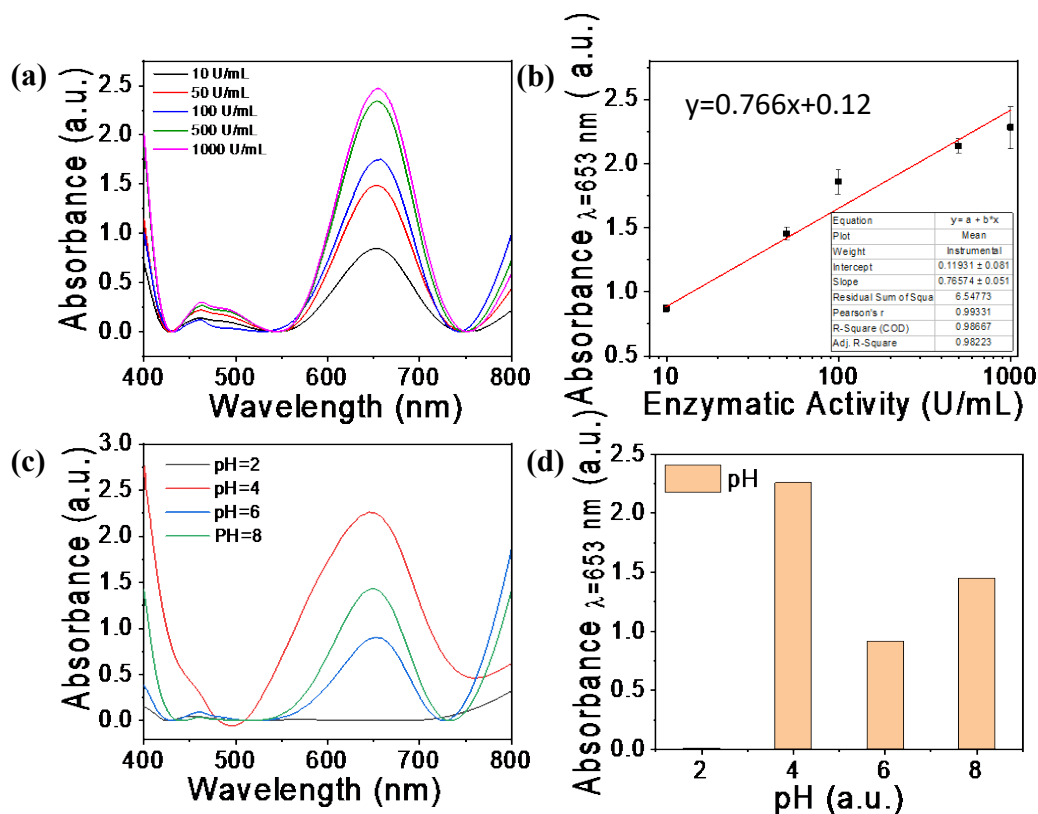
2. Catalytic performance of GOx



Supplemental Figure 5: Related to Figure 2

Figure S5. The photograph under control vs nanoreactor (a) and the pH=4.0, 7.4, respectively (c). UV-vis absorption spectra of the oxidized TMB (oxTMB) produced under control vs nanoreactor (b) and the pH=4.0, 7.4, respectively (d).

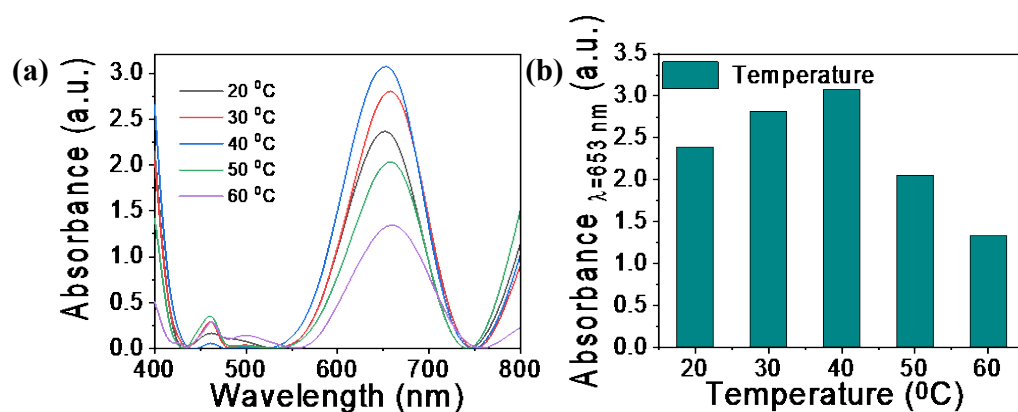
In order to find the pH value with the best catalytic activity of GOx, we firstly conducted a chromogenic reaction of tetramethyl benzidine (TMB) under different enzyme activities of GOx and obtained a good linear response to GOx activity in a range from 10 to 1000 U/mL (Figure S6b) with regression equation of $y=0.766x+0.12$. Then, the UV-vis absorption spectra of the oxidized TMB (oxTMB) produced under different pH were carried out. According to the Figure S6c&d, the optimum pH for GOx activity is ~ 4 in vitro and the activity of GOx is about 616.6 U/mL in the acidic environment of the tumor.



Supplemental Figure 6: Related to Figure 2

Figure S6. (a) UV-vis absorption spectra of the oxidized TMB (oxTMB) produced under different enzyme activities of GOx. (b) The plot of the absorbance intensity at 653 nm with the enzyme activities of GOx. (c) UV-vis absorption spectra of the oxidized TMB (oxTMB) produced under different pH and (d) corresponding histogram of absorbance intensity at 653 nm vs pH.

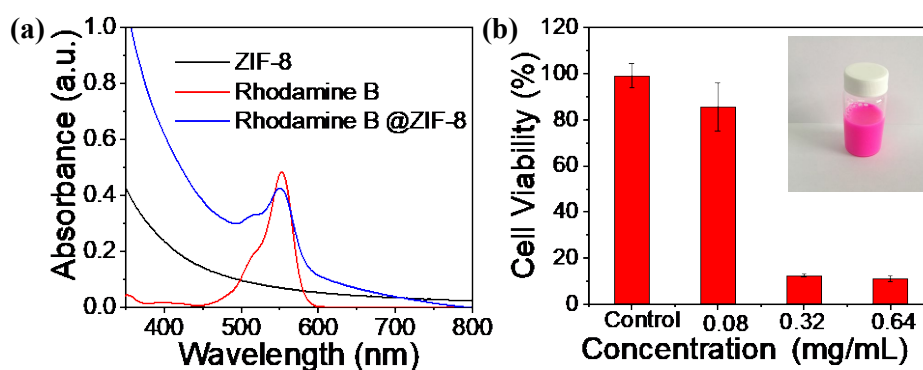
To prove whether the activity of GOx is affected by 5% SDS (w/w) aqueous solution at 50°C, we determined the UV-vis absorption spectra of the oxidized TMB (oxTMB) produced under different temperature. As shown in Figure S7a&b of revised supporting information, GOx maintained 85.8% activity at 50°C compared to room temperature.



Supplemental Figure 7: Related to Figure 2

Figure S7. (a) UV-vis absorption spectra of the oxidized TMB (oxTMB) produced under different temperature and (b) corresponding histogram of absorbance intensity at 653 nm vs temperature.

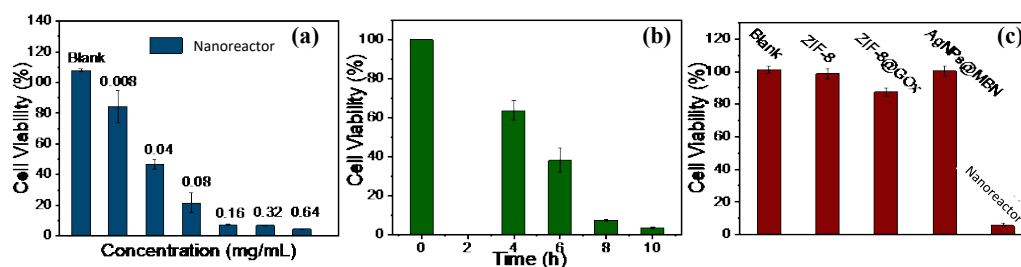
3. Characterizations of ZIF-8@RhB



Supplemental Figure 8: Related to Figure 2

Figure S8. (a) UV-vis absorption spectra of ZIF-8, Rhodamine B (RhB) and RhB@ZIF-8, respectively. The absorption band at 552 nm is originated from RhB. (b) Cell viabilities of different concentrations RhB@ZIF-8 pretreated HeLa cells for 24 h, determined by the standard MTT assay, showing that an optimized concentration is 0.08 mg/mL. The inset shows a photograph of RhB@ZIF-8.

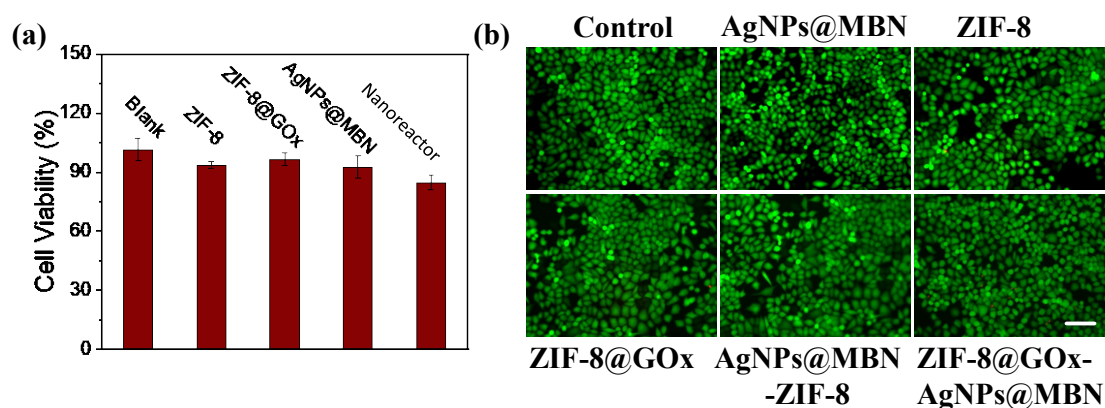
4. Treatment effect of the nanoreactor for HeLa cells



Supplemental Figure 9: Related to Figure 3

Figure S9. (a) HeLa cells viabilities incubated with different concentrations of the ZIF-8@GOx-AgNPs@MBN nanoreactors. (b) Cell viabilities of the nanoreactor (0.8 mg/mL)-pretreated HeLa cells for different incubation time. (c) The viability of the HeLa cells treated with different nanoparticles, including blank, ZIF-8, ZIF-8@GOx, AgNPs@MBN and the ZIF-8@GOx-AgNPs@MBN nanoreactors.

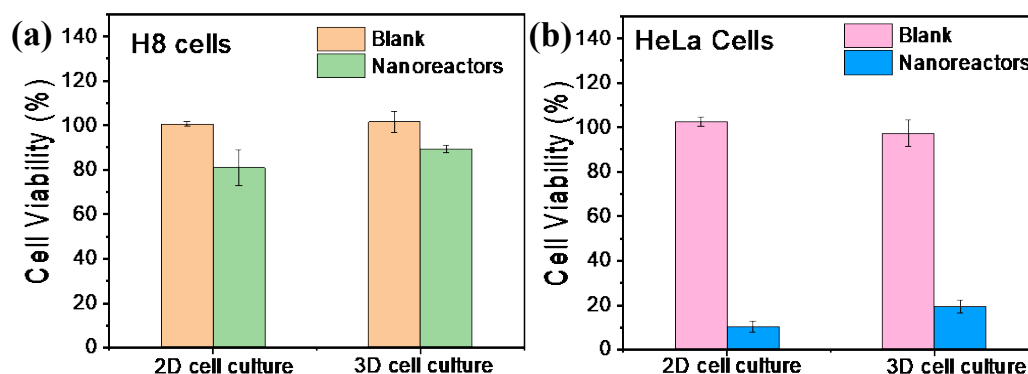
5. Cell viabilities of H8 cells under different treatments



Supplemental Figure 10: Related to Figure 3

Figure S10. (a) The cell viability of H8 cells after the treatment with different nanomaterials, including control, ZIF-8, ZIF-8@GOx, AgNPs@MBN and ZIF-8@GOx-AgNPs@MBN. (b) The corresponding fluorescent images of H8 cells underwent different treatments (cells were stained by Calcein-AM/PI; green, alive; red, dead). All of the scale bars are 60 μ m.

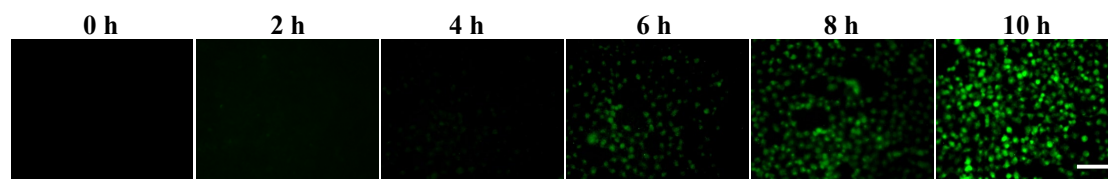
6. Comparison of H8 cells viability under 2D and 3D cell culture



Supplemental Figure 11: Related to Figure 3

Figure S11. The viability of H8 cells (a), HeLa (b) under 2D and 3D cell culture. The concentration of the nanoreactor used is 0.8 mg/mL, and incubation time is 8 h.

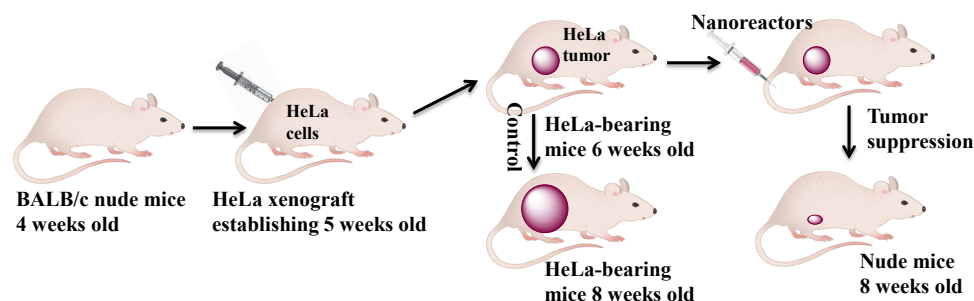
7. Evaluation of H₂O₂ content in HeLa cells



Supplemental Figure 12: Related to Figure 3

Figure S12. The confocal fluorescent images of HeLa cells after co-incubation with the ZIF-8@GOx-AgNPs@MBN nanoreactors for different periods. All of the scale bars are 50 μ m. Cells were stained with RDPP [Ru(dpp)₃]Cl₂.

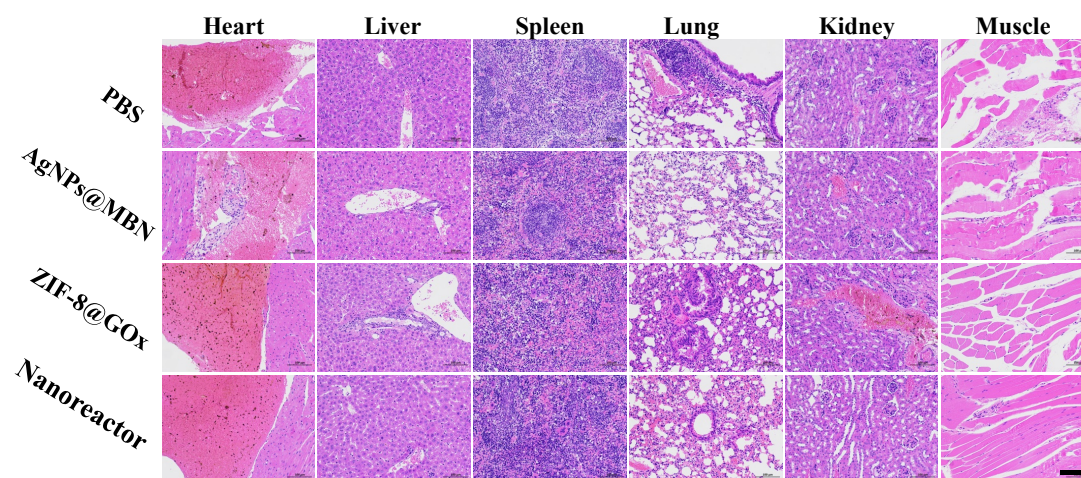
8. Establishment of cervical tumor xenograft



Supplemental Figure 13: Related to Figure 4

Figure S13. Schematic illustration of the cervical tumor xenograft establishment, blank and synergistic chemo-starving cancer therapy procedures, and therapeutic outcome.

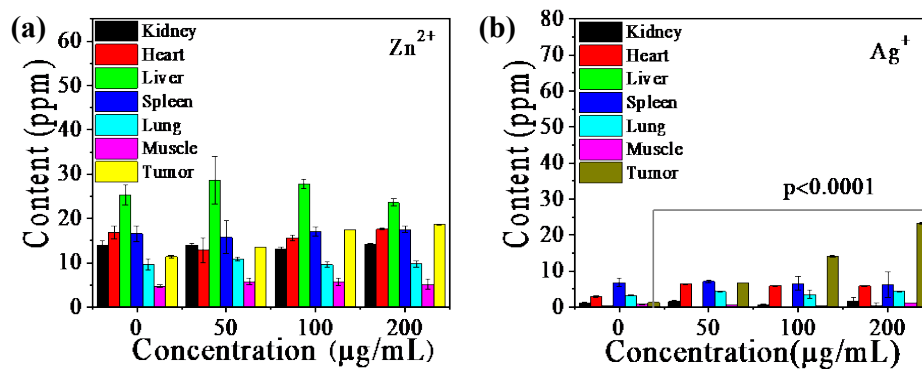
9. H&E staining of main organs



Supplemental Figure 14: Related to Figure 5

Figure S14. H&E staining images of the main organs after the different treatments. All of the scale bars are 100 μm .

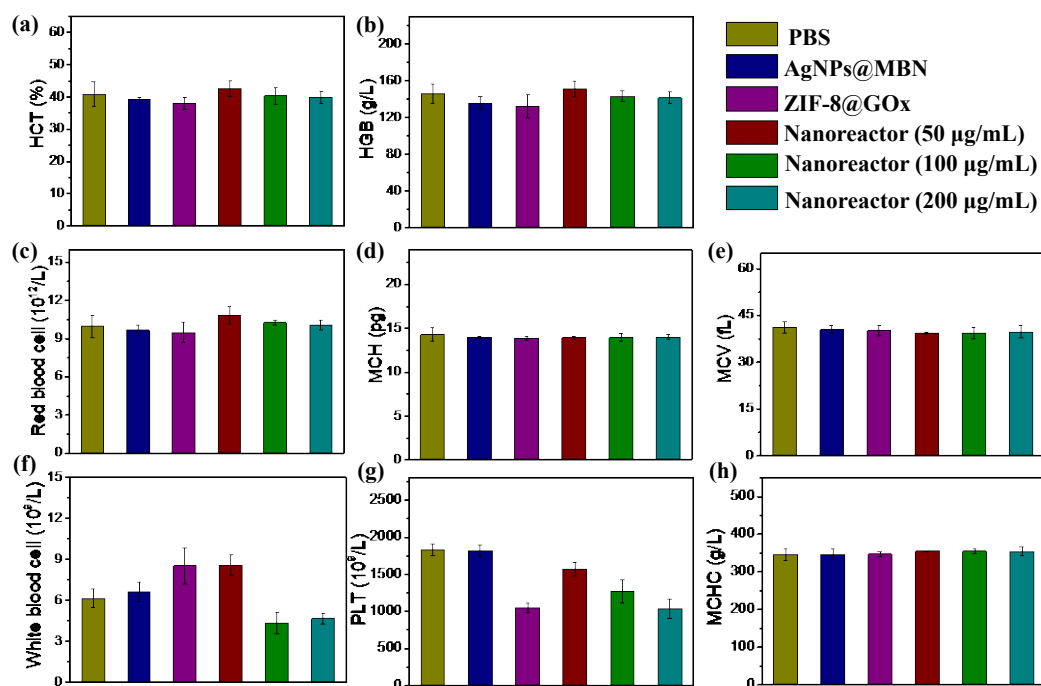
10. Biodistributions of Zn^{2+} and Ag^+ in main organs



Supplemental Figure 15: Related to Figure 5

Figure S15. Biodistributions of Zn^{2+} (a) and Ag^+ (b) in main organs and tumors on the 14th day of intravenous administrations of the nanoreactors with different dosages.

11. Blood chemistry analyses of the tested mice



Supplemental Figure 16: Related to Figure 5

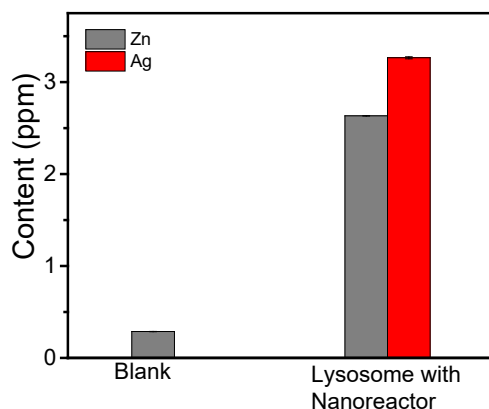
Figure S16. (a) HCT, (b) Hemoglobin, (c) RBC, (d) MCH, (e) HCV, (f) WBC, (g) PLT and (h) MCHC levels of the tested mice in all groups. Mean values and error bars are from three trials.

Supplemental Table 1: Related to Figure 5

Table S1: The trace element levels of mice in all groups. Each sample is measured three times.

	Pb (µg/L)	Zn (µmol/L)	Cu (µmol/L)	Fe (mmol/L)	Ca (mmol/L)	Mg (mmol/L)
PBS	44	56.58	22.90	7.12	1.74	1.58
AgNPs@MBN	42	58.79	13.60	7.24	1.68	1.58
ZIF-8@GOx	38	60.7	13.42	7.83	1.44	1.46
Nanoreactor (50 µg/mL)	28	58.12	23.93	7.34	1.65	1.61
Nanoreactor (100 µg/mL)	29	66.88	21.85	7.84	1.77	1.65
Nanoreactor (200 µg/mL)	29	56.68	20.59	7.13	1.60	1.52

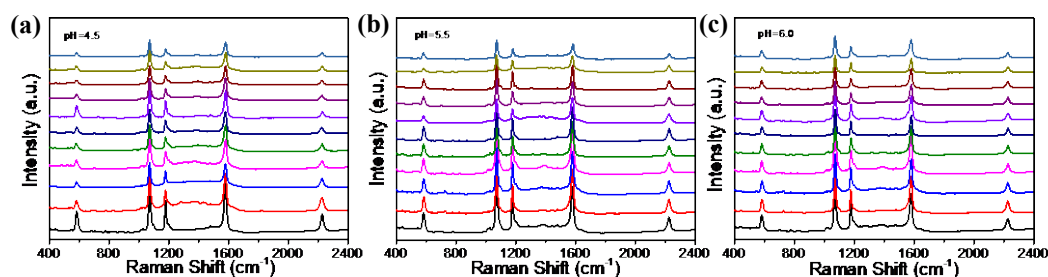
12. Biodistributions of Zn^{2+} and Ag^+ in extracted lysosomes



Supplemental Figure 17: Related to Figure 5

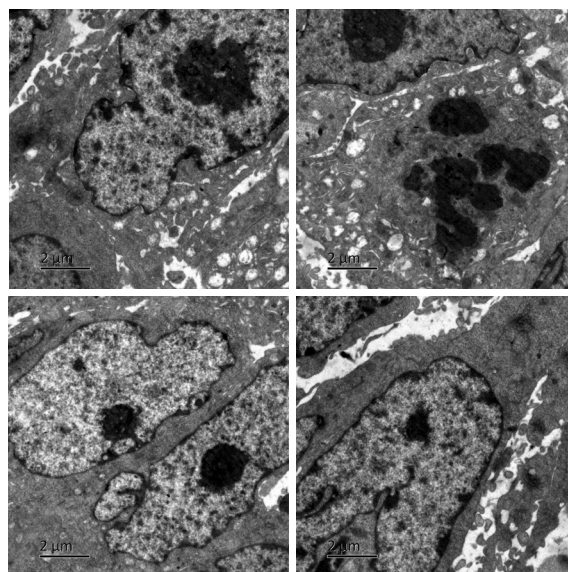
Figure S17. Comparison of the biodistributions of Zn^{2+} and Ag^+ in blank and extracted lysosomes with the nanoreactors.

13. GOx release self-sensing



Supplemental Figure 18: Related to Figure 5

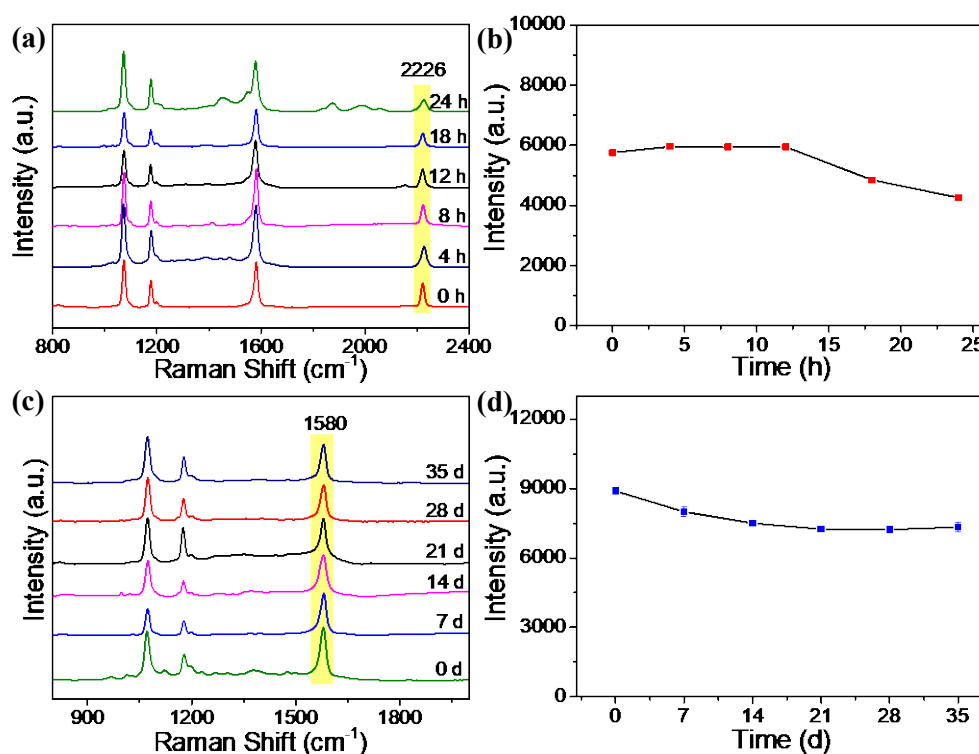
Figure S18. SERS spectra of MBN on the nanoreactors after they reacted with 5.0 mM of glucose at different pHs of 4.5 (a), 5.5 (b), and 6.0 (c) with different reaction time (0-5 h), recorded every 0.5 h.



Supplemental Figure 19: Related to Figure 5

Figure S19. Bio-TEM images of the tumor tissues after 14 d postinjection of the nanoreactor.

14. Long-term stability of the nanoreactor



Supplemental Figure 20: Related to Figure 5

Figure S20. (a) SERS spectra of MBN on the nanoreactor kept in 50% serum at 37 °C for different time (0, 4, 8, 12, 18 and 24 h). (b) SERS intensity variation at 2226 cm⁻¹ with different incubation time. SERS spectra (c) and intensity at 1580 cm⁻¹ (d) of the nanoreactor along with the

storage time (at 4 °C), recorded every one week.

This nanoreactor keeps long-persistent activity under the 4 °C storage for at least one month (Figure S20).

Transparent Methods

Materials and Instrument

4-mercaptobenzonitrile (MBN) was purchased from Nanjing Shengsai Chemical Co., Ltd. 3-(4, 5-Dimethylthiazol-2-yl)-2, 5-diphenyltetrazolium bromide (MTT) and dimethyl sulfoxide (DMSO) were bought from Key-GenBioTech. Hexahydrate and zinc nitrate ($\text{Zn}(\text{NO}_3)_2 \cdot 6\text{H}_2\text{O}$), 2-methylimidazole, sodium chloride (NaCl), potassium chloride (KCl), Calcein-AM/ propidium iodide (PI), sodium borohydride (NaBH_4), sodium citrate ($\text{C}_6\text{H}_5\text{Na}_3\text{O}_7$), glucose oxidase (GOx), silver nitrate (AgNO_3), adenosine triphosphate (ATP), alkaline phosphatase, troponin, prostate specific antigen (PSA), cytochrome c, trypsin, glutathione (GSH) and glucose were purchased from Aladdin Industrial Corporation (Shanghai, China). Caspase-3 was purchased from the Wuhan Cloud Clone Corp. Hoechst 33342 and LysoSensor™ Green were obtained from Invitrogen (Carlsbad, CA). Rhodamine B (RhB) and sodium dodecylsulfate ($\text{CH}_3(\text{CH}_2)_{11}\text{OSO}_3\text{Na}$) were bought from Beijing Chemical Works. 7-AAD/Annexin-V-APC was purchased from the Thermo Fisher Scientific Biological Co., Ltd. The Dulbecco's modified Eagle's medium (DMEM), antibiotic solution, fetal bovine serum (FBS) and 0.25% trypsin/2.2 mM EDTA solution were purchased from Biological Industries. The lysosomal extraction kit was purchased from Sigma-Aldrich (USA). All the solutions were prepared through the ultrapure water (DI water) which was obtained using a Millipore Milli-Q water purification system (Billerica, MA), with an electric resistance $>18.25 \text{ M}\Omega$.

The morphologies of the ZIF-8 and AgNPs were characterized by the transmission electron microscope (TEM, Hitachi 600), and their composite was imaged by the high-angle annular dark-field (HAADF)-STEM and elemental mapping. The UV-vis absorption spectra were obtained with a Lambda 750 spectrophotometer (Perkin-Elmer). The concentrations of the nanoreactors and metal elements were detected using the inductively coupled plasma mass spectrometry (ICP-MS, Thermo Scientific Icap 6300). The dynamic light scattering (DLS, Zetasizer Nano ZS 90,

British Ma Erwen Co., Ltd.) was used for the Zeta potential measurements. The chemical compositions of the samples were conducted by X-ray photoelectron spectroscopy (XPS) (Escalab 250Xi, Thermo Fisher Scientific). The X-ray Irradiator (D8 Advance) was from the Bruker. The living cell fluorescent images were performed with an inverted microscope (Leica DMI6000B, Germany). The Fourier transform infrared (FTIR) spectrum was performed using a Bruker Vertex 80 V spectrometer. SERS measurements were carried out using a Horiba Jobin Yvon Aramis spectrometer at 632.8 nm from a laser power of ~7 mW and an accumulation time of 5 s per time. Thermo gravimetric analysis (TGA) was performed using a TG 209 F1 Libra thermal gravimetric analyzer (Netzsch, Germany). Flow apoptosis assay was carried out using a BD FACSCanto II analytical flow cytometry.

Synthesis of the ZIF-8 nanoparticles (NPs)

The ZIF-8 nanocrystals were prepared using the previously reported work (Pan et al., 2011). Firstly, the two solutions were all filtered by filter paper before mixing. Typically, 1.17 g of zinc nitrate (3.95 mmol) in 8 mL DI water was added into a solution of 2-methylimidazole (22.70 g, 276.50 mmol) in 80 mL of DI water to ensure the molar ratio of 2-methylimidazole to zinc as 70:1. Then, the product was collected by repeated centrifugation (8000 rpm, 10 min) and wash by DI water for three times.

Preparation of glucose oxidase (GOx) payloaed ZIF-8 NPs

Firstly, 0.117 g of zinc nitrate was dissolved into 0.8 mL of DI water, and then 10 mg of GOx was added into the zinc nitrate solution to stir for 10 min at 30°C. After that, 2.27 g of 2-methylimidazole in 8 mL of DI water was added into the mixed solution under vigorous stirring and incubated at 30°C for 10 min. The resulting GOx payloaed ZIF-8 NPs (ZIF-8@GOx) were centrifuged at 8000 rpm for 10 min, followed by twice wash with DI water. They were then cleaned by a 5% SDS (w/w) aqueous solution at 50 °C to remove free GOx on the surface. Finally, the ZIF-8@GOx NPs were stored in 4°C for use.

Synthesis of AgNPs and AgNPs@MBN

The AgNPs were prepared according to the reported literature (Agnihotri et al., 2014). Typically, the fresh aqueous solution of NaBH₄ (1.00 mM, 1.0 mL) and sodium citrate (3.55 mM, 1.0 mL) were added into 93.0 mL of DI water to stir at 60 °C in the dark for 30 min. Next, 1.0 mL of AgNO₃ (1.00 mM) was added drop-wise to the mixture. Subsequently, the temperature was raised to 90 °C and then the pH of the solution was adjusted to 10.5 by NaOH (0.1 M). The solution was kept boiling for 20 min until the solution color changed to greyish green. The AgNPs were centrifuged three times at 12000 rpm for 10 min, and finally re-dispersed into DI water and stored at 4 °C for use.

MBN was chosen as the Raman reporter. 4-MBN were conjugated to AgNPs via the Ag-S bond. Briefly, 100 μL of 2mM 4-MBN were added to 2 mL AgNPs, followed by incubation for 24 h. Excess 4-MBN were then removed by centrifugation at 12000 rpm for 10 min. The resultant 4-MBN-modified AgNPs were washed and re-dispersed in deionized water.

Preparation of nanoreactor

The nanoreactors were fabricated *via* the electrostatic assembly of the ZIF-8@GOx NPs and the AgNPs@MBN since their surface charges are adverse according to the Zeta potential characterization (Fig. 1g). In a typical preparation, 1.0 mL of ZIF-8@GOx NPs (0.8 mg/mL) was mixed with 10 mL of AgNPs@MBN (2.5×10^{-5} M) and the mixture was kept stirring for 24 h. Subsequently, the nanoreactors of ZIF-8@GOx-AgNPs were three times centrifuged at 7000 rpm for 10 min to remove free AgNPs@MBN and the produced nanoreactors were then stored in 4 °C for use.

Catalysis ability of the nanoreactor for glucose *ex vivo*

The nanoreactor can start to an acid-responsive catalytic cascade reaction, which can be self-sensed by the AgNPs@MBN element on the nanosensor. The sensing mechanism is as follows: a lower pH environment causes the damage of ZIF-8 cages,

making the leakage of GOx from the cages. In the appearance of glucose, the released GOx reacts with glucose to produce H₂O₂ and D-gluconic acid (Reaction 1). One of the catalysis products, H₂O₂, can induce a “turn-off” mechanism of the SERS intensity of the Raman reporter (MBN) laid on AgNPs due to the etching effect on AgNPs.

The SERS intensity of the AgNPs@MBN nanoprobe before and after the nanoreactors reacted with glucose was tracked, and the catalysis abilities under different pHs were compared by the changes of their SERS intensities. The prepared nanoreactor was centrifuged at 7000 rpm for 10 min and re-dispersed in PBS solutions with the pHs of 4.5 and 7.0, respectively. Then, a glucose solution (5 mM, 20 μ L) was added into 200 μ L of the nanoreactor solution (0.8 mg/mL) and the catalysis reaction between GOx and glucose was carried out in 37°C for 3 h. Next, we dripped 10 μ L of the resulting solution onto a glass slide for SERS measurements to trace the catalysis activity of GOx under an acid condition, and the results of which are shown in Figure 2a.

Next, we optimized the detection sensitivity of the nanoreactor *ex vivo*. In the assay, 200 μ L of the nanoreactor PBS solution (0.8 mg/mL, pH=4.5) was mixed with 20 μ L of different concentrations of glucose (0-10 mM) and the mixtures were incubated at 37°C for 3 h. The SERS measurements are as same as described above and the results are presented in Figure 2b. We plotted the peak intensities at 2226 cm⁻¹ with the glucose concentration and a linear fitting curve was obtained as shown in Figure 2b. It gives a fitting equation as $y=0.1605+0.0419 x$, with a $R^2=0.9254$.

Cell culture

HeLa (cervical cancer cell line) and H8 (cervical epithelial immortalized cell line) cells were bought from the American Type Culture Collection (ATCC, USA). The two cell lines were cultured in the Dulbecco's Modified Eagle's Medium (DMEM) supplemented with 10% fetal bovine serum (FBS), 100 U/mL penicillin, and 100 μ g/mL streptomycin at 37°C in a humidified atmosphere containing 5% CO₂.

Internalization of nanoreactors in cells

HeLa cells (or H8 cells) at a density of 1×10^5 cells per mL were planted into 35 mm culture dishes for 12 h, and then they were incubated with the nanoreactors (20 μ L, 0.8 mg/mL) at 37 °C for 6 h (different culture time were also tried as 0, 2, 4 and 6 h). After that, the mediums were removed and the cells were gently washed three times with PBS.

Intracellular glucose determination by the nanoreactor

To confirm the glucose consumption in cells, the HeLa cells with nanoreactors in one dish were fixed by 4% formaldehyde every one hour, and totally, eight samples representing 0-7 h of the reaction time were achieved. The SERS spectra of the SERS nanoprobe on the endocytosed nanoreactors were recorded on the fixed cells, which can report the intracellular glucose amount during the different treatment stages, as shown in Figure 3d.

Rhodamine B-encapsulated ZIF-8 NPs for living cell imaging

To achieve the location information of the nanoreactors within cells, we prepared the RhB/ZIF-8 NPs and characterized them with a confocal laser scanning microscope (CLSM). In a typical preparation, 0.117 g of zinc nitrate was dissolved into 0.8 mL of DI water, while 0.1 mg of rhodamine B (RhB) was added into the zinc nitrate solution to stir at 30 °C for 10 min. Then, 2.27 g of 2-methylimidazole in 8 mL of DI water was added into the mixed solution under vigorous stirring for another 10 min. The resulting RhB-encapsulated ZIF-8 NPs were centrifuged at 8000 rpm for 10 min and washed with DI water.

The HeLa cells (1×10^5 cells/mL) were cultured with 0.8 mg/mL of the ZIF-8@RhB NPs. The internalization of the nanoreactors can be controlled by different incubation time (0, 2, 4 and 6 h). Subsequently, the cells were washed again by the cold PBS and then they were stained with LysoSensor™ Green (2.5 μ g/mL) for 20 min. After three times washing, the cells were observed by the CLSM with a 40 \times objective.

Cell viability assay

The cell viability test was performed with the standardized MTT (3-(4,5-dimethylthiazol-2-yl)-2,5-diphenyltetrazolium bromide) assay. Typically, the cells were seeded on the 96-well microtiter plates for 12 h incubation at 37 °C. Then, the cells were washed three times using the cold PBS. Different concentrations of ZIF-8@GOx-AgNPs@MBN NPs were added into each well, supplemented with the complete medium to 100 µL, and then they were cultured at 37 °C for another 24 h. After the cells were washed with the cold PBS, 5 µL of the MTT solution (5.0 mg/mL) was added into each well for additional 4 h at 37 °C. Finally, after removing the medium, 150 µL of DMSO was added into each well to dissolve the purple formazan crystal. The absorbance of each well was measured at 570 nm by a microplate reader and the MTT results are shown in Figure S7a.

Also, we assessed the cell viabilities of HeLa cells by the MTT assay when the cells were cultured with Ag⁺, Zn²⁺, Ag⁺/Zn²⁺, with or without glucose (5 mM) for 24 h. The results are displayed in Figure 3e and 3f.

Live/dead cell staining

The cells (seeded density is 1×10⁵ cells/mL) were stained with calcein-AM (2 µM) and propidium iodide (PI, 4 µM) for 20 min. Finally, the stained cells were washed three times using the PBS and they were imaged by using a Leica DMI6000B microscope with a 10× objective (Figure 3c).

For a comparison, PBS (control), ZIF-8, ZIF-8@GOx (0.8 mg/mL), and AgNPs@MBN (2.5 × 10⁻⁵ M) were also used instead of the ZIF-8@GOx-AgNPs@MBN for assessing their therapeutic effects (Figure 3c).

Evaluation H₂O₂ content change within HeLa cells

RDPP [Ru(dpp)₃]Cl₂ as a hydrogen peroxide fluorescence-specific probe (Qi et al., 2019), with a concentration of 0.3 µM, was incubated with the nanoreactors internalized HeLa cells for 30 min. Finally, the cells were washed with PBS three

times and the hydrogen peroxide highlighted by RDPP in the cells was observed under a fluorescence microscope (Leica DMI6000B, Germany) with a 20× objective.

Cell apoptosis assay by flow cytometry

For apoptosis analysis by flow cytometry, the HeLa cells were seeded in the 6-well plates at a density of 1×10^5 cells/well and grown overnight in 5% CO₂ at 37 °C. The adherent cells were treated by the nanoreactors (20 μL per well, 0.08 mg/mL) at 37 °C for different time (0, 2, 4, 6, 8, and 10 h, respectively). The cells were collected by 4 min of cell dissociation and centrifugation (1500 rpm, 3 min) followed twice PBS washing. Then, 200 μL of the binding buffer was added to re-disperse the HeLa cells. Annexin-V-APC (5 μL) and 7-AAD (5.0 μL) were added and cultured for 30 min, which can stain the live and dead cells according to the instructions. Finally, the flow cytometer was operated to detect cell apoptosis after the treatments.

Bio-TEM imaging of cells

The HeLa cells were incubated with 0.08 mg/mL of the nanoreactor in a DMEM medium in 5% CO₂ at 37 °C for 6, 12, 24 h, respectively. Then, they were washed twice using cold PBS (pH = 7.4) and detached by incubation with 0.25% of trypsin. The cell suspension was centrifuged at 1500 rpm for 3 min. After removing the culture medium, the cells were washed twice with PBS. The cells were fixed by glutaraldehyde at 4 °C. The sample was rinsed with PBS and dehydrated by a graded ethanol series. The samples were then embedded in EPOM812 and polymerized in the oven at 37 °C for 12 h, 45 °C for 12 h and 60 °C for 48 h. The fixed sample was cut into many ultrathin sections with approximately 70 nm in thickness by a diamond knife on a Leica UC6 ultramicrotome. The sample sections were transferred to the copper grids and imaged on a JEM-1230 transmission electron microscope.

Animal experiments

BALB/c nude mice (four weeks old, 18 ± 0.2 g, female) were purchased from Beijing

HFk Biotechnology Ltd. (Beijing, China). Animal care and handling procedures were in agreement with the guidelines of the Regional Ethics Committee for Animal Experiments.

Tumor models and *in vivo* chemo-starvation therapy

The 50 μL of cell contained PBS solution (5×10^6 cells/mL) was injected into each mouse subcutaneously. The mice were applied for further experiments when the tumor had grown to 8-10 mm in diameter. Then, the mice were divided into six groups at random for the treatments with the following nanomedicines: control (PBS), AgNPs@MBN, ZIF-8@GOx and the nanoreactor of different concentrations (50, 100, and 200 $\mu\text{g}/\text{mL}$, respectively), with three mice set as one group. Above nanomedicines were injected intravenously into the mice.

To monitor the therapeutic effects of different nanomedicines, we measured the tumor size by using the digital caliper in two dimensions to calculate the tumor volume according to the following equation: Tumor volume = (length \times width²)/2. Meanwhile, the body weight changes of mice were recorded every day to estimate the efficacy of physical recovery. On the 14th day, the tumors were weighed to assess the therapeutic efficacy of different experimental groups.

***In vivo* biocompatibility evaluation**

For *in vivo* biosafety evaluation, female nude mice were separated into six groups (n = 6) randomly when they were four weeks old, and they were treated with the control, AgNPs@MBN, ZIF-8@GOx and the nanoreactor at different concentrations (50, 100, 200 $\mu\text{g}/\text{mL}$, respectively). After a 14-day period, all nude mice were dissected to collect their organs (tumor, heart, liver, spleen, lung, kidney and muscle). The organs were cut into thin slides and fixed by paraformaldehyde (4 wt%) for the hematoxylin and eosin (H&E) staining assay. The blood samples of each experimental group including the control group were collected at the same time. Then, we measured the trace elements in the blood samples, including Pb, Zn, Cu, Fe, Ca and Mg. The Zn^{2+}

and Ag^+ contents in the above major organs were analyzed by the ICP-MS (Figure 4h and 4i), which can reveal the metabolism ways of Zn^{2+} and Ag^+ *in vivo*.

***In vivo* SERS detection**

The BALB/c mice were received 200 $\mu\text{g}/\text{mL}$ of the nanoreactor per kg by intravenous injection when the tumor reached 8-10 mm in diameter. The mice with 24 h and 14 d post-injection were anesthetized and examined under a confocal Raman spectrometer with 20 mW laser power at 785 nm (Figure 5g). The laser beam was focused on the tumors or normal muscles with a focal distance of ~ 9 mm. Thus, SERS spectra were obtained in a completely noncontact and noninvasive manner.

Lysosome extraction of HeLa cells incubated with the nanoreactor

The lysosome extraction from HeLa cells was performed directly after the incubation with the nanoreactors for 6 h according to the protocol indicated in the lysosomal extraction kit. Briefly, cells ($\sim 1 \times 10^6$ cells/mL) were centrifugated at $500 \times g$ rpm for 5 min under 4°C to remove the culture medium and washed using a cold PBS solution twice. After that, the cold extraction A of 400 μL was adding into the cells on the ice for 10 min and using the homogenizer for 20-40 cycles of homogenization. Then, the gradient centrifugation of the cells was carried out at 4°C (: 1000 rpm for 5 min, 3000 rpm for 10 min, 5000 rpm for 10 min, 20000-30000 rpm centrifugation, 20 min) and the supernatant was kept each time by transferring to a new cold tube, except the precipitates were kept for the last high-speed centrifugation. Then, 400 μL of the cold extraction B were added, then the mixture was centrifugated under 20000-30000 rpm for 20 min at 4°C and the precipitates were the lysosomes with the nanoreactors.

References:

Agnihotri, S., Mukherji, S., and Mukherji, S. (2014). Size-controlled silver nanoparticles synthesized over the range 5-100 nm using the same protocol and

their antibacterial efficacy. *RSC Adv.* *4*, 3974–3983.

Pan, Y.C., Liu, Y.Y., Zeng, G.F., Zhao, L., and Lai, Z.P. (2011). Rapid synthesis of zeolitic imidazolate framework-8 (ZIF-8) nanocrystals in an aqueous system. *Chem. Commun.* *47*, 2071–2073.

Qi, G.H., Zhang, Y., Wang, J.F., Wang, D.D., Wang, B., Li, H.J., and Jin, Y.D. (2019). Smart plasmonic nanozyme enhances combined chemo-photothermal cancer therapy and reveals tryptophan metabolic apoptotic pathway. *Anal. Chem.* *91*, 12203–12211.